

Article

# Hyperspectral Estimation of the Chlorophyll Content in Short-Term and Long-Term Restorations of Mangrove in Quanzhou Bay Estuary, China

Zhiguo Dou <sup>1,2,3</sup> , Lijuan Cui <sup>1,2,3</sup>, Jing Li <sup>1,2,3</sup>, Yinuo Zhu <sup>1,2,3</sup>, Changjun Gao <sup>4</sup>, Xu Pan <sup>1,2,3</sup>, Yinru Lei <sup>1,2,3</sup> , Manyin Zhang <sup>1,2,3</sup>, Xincheng Zhao <sup>1,2,3</sup> and Wei Li <sup>1,2,3,\*</sup> 

<sup>1</sup> Institute of Wetland Research, Chinese Academy of Forestry, Beijing 100091, China; linqudouzhiguo@126.com (Z.D.); wetlands108@126.com (L.C.); lijinghznd@126.com (J.L.); zhuwen\_100@163.com (Y.Z.); xu\_pan\_decom@126.com (X.P.); leiyinru@126.com (Y.L.); cneco@126.com (M.Z.); surezx4@163.com (X.Z.)

<sup>2</sup> Beijing Key Laboratory of Wetland Services and Restoration, Beijing 100091, China

<sup>3</sup> Beijing Hanshiqiao National Wetland, Ecosystem Research Station, Beijing 101399, China

<sup>4</sup> Guangdong Academy of Forestry, Guangzhou 510520, China; gaochangjun015@163.com

\* Correspondence: wetlands207@163.com

Received: 25 January 2018; Accepted: 5 April 2018; Published: 9 April 2018



**Abstract:** The chlorophyll content can indicate the general health of vegetation, and can be estimated from hyperspectral data. The aim of this study is to estimate the chlorophyll content of mangroves at different stages of restoration in a coastal wetland in Quanzhou, China, using proximal hyperspectral remote sensing techniques. We determine the hyperspectral reflectance of leaves from two mangrove species, *Kandelia candel* and *Aegiceras corniculatum*, from short-term and long-term restoration areas with a portable spectroradiometer. We also measure the leaf chlorophyll content (SPAD value). We use partial-least-squares stepwise regression to determine the relationships between the spectral reflectance and the chlorophyll content of the leaves, and establish two models, a full-wave-band spectrum model and a red-edge position regression model, to estimate the chlorophyll content of the mangroves. The coefficients of determination for the red-edge position model and the full-wave-band model exceed 0.72 and 0.82, respectively. The inverted chlorophyll contents are estimated more accurately for the long-term restoration mangroves than for the short-term restoration mangroves. Our results indicate that hyperspectral data can be used to estimate the chlorophyll content of mangroves at different stages of restoration, and could possibly be adapted to estimate biochemical constituents in leaves.

**Keywords:** chlorophyll content; hyperspectral; estimation model; mangrove

## 1. Introduction

Mangroves grow along the edges of harbors and beaches in tropical and subtropical areas. As fixed “coastguards”, mangroves have adapted to the harsh, oxygen-deficient, and highly saline conditions, and they play important roles in maintaining the ecological balance, stabilizing beaches and embankments, and purifying water [1,2]. China’s mangrove forests have been devastated since the beginning of the 1950s, when China began to reclaim land from the sea and deforest mangroves to farm fish and shrimp and build wharfs. By 1994, the total area of mangrove forests in China was less than 15,000 hm<sup>2</sup>, which was less than one-third of the area at the historical peak of mangrove resources [3]. In the past 20 years, the ecological functions of mangroves, and the need to manage and protect them, have gradually been recognized. China has implemented various projects to conserve and restore mangroves, and, with large-scale ecological restoration work under way, the area of mangrove forest is

expected to reach 70,000 hm<sup>2</sup> by 2020 [4]. The chlorophyll content is an indicator of vegetation stress and can be used as a basis for estimating other biochemical parameters [5] and should be measured when monitoring, restoring and managing coastal wetland ecosystems. As such, it would therefore be useful if there were methods that resource managers could use to monitor the chlorophyll content of mangroves from hyperspectral data [6–9].

Mangroves adapt to high-salt habitats using a range of physiological, biochemical, and morphological mechanisms. It is generally accepted that mangroves fall into two types, namely salt-secreting species with salt glands and salt-excluding species without salt glands [10,11]. *Aegiceras* plants have salt glands that secrete Na and Cl through their leaves to maintain the salt balance while *Kandelia* plants are known as salt-rejecting mangrove species that isolate the matrix from salt water mainly through high negative pressure in the xylem [12,13]. The mechanisms used by mangroves are unique within the plant kingdom, and the two different survival modes of mangroves have led to some differences between the leaves of the two mangrove species. The growth and physiological metabolism of mangroves are distinctive during different stages of restoration [14,15]. To date, hyperspectral data have not been used to compare the growth of these two mangrove species at different stages of restoration; instead, remote sensing has been used frequently to classify mangrove species and estimate biomass [16–20]. For example, Jia et al. mapped the Maipu mangrove species using hyperspectral data from the EO-1 HYPERION sensor [21]. After applying analysis of variance to hyperspectral data collected from mangrove leaves under laboratory conditions, Vaiphasa et al. identified sixteen mangrove species [22]. The chlorophyll content has also been used to indicate how oil pollution and seasonal stress to mangroves [23,24]. Flores-de-Santiago estimated the chlorophyll content in mangroves in different seasons from hyperspectral data to determine the optimal time for monitoring [25]. Other studies have evaluated ecosystems services, determined the biomass, and quantified physical and chemical parameters, including nutrients, of mangrove forests at different stages of restoration, but only a few studies have considered the chlorophyll content of mangroves [26–29].

In recent years, methods for estimating the chlorophyll content from hyperspectral data have improved considerably. The chlorophyll content is generally estimated using regression analysis, physical modeling, or spectral parameters. Of these, the spectral parameter method is widely used as the physical mechanisms are considered when constructing the index and it only uses a narrow observation band [5,30]. All spectral indices are affected by many factors, such as the vegetation type, development stage, and background environment [31,32]. The sensitivity of, and inherent theoretical explanations for, the different vegetation and growth stages need further research. At present, the red-edge position model is the most mature model for estimating the chlorophyll content. In the plant spectrum, the green plant reflectivity between 680 and 760 nm increases most rapidly at what is called the red edge. The red edge is produced because of the transition from vegetation's red band absorption of chlorophyll to multiple scattering of near-infrared light. Because of its ability to indicate plant pigments and health, and its close relationship with the chlorophyll content of plants, the red edge is an effective tool for assessing the vegetation status by remote sensing [33–35]. Many scholars, from studies of the relationship between the red edge and the chlorophyll content, have shown that the chlorophyll content can be estimated from the red edge [36]. Dawson examined the relationship between the leaf area index (LAI) and the position of the red-edge, and found that there was a strong nonlinear relationship between the LAI and the red-edge position [37]. Curran obtained the optimal red-edge band for estimating the chlorophyll content by establishing a relationship between the red-edge position and reflectivity at different wavelengths [38]. Flores-de-Santiago and Zhang et al. suggested that wavebands at the red edge position were the best predictors of the pigment contents [24,39].

Hyperspectral remote sensing has been used successfully to monitor the restoration of ecosystems; for example, vegetation abundance and vegetation succession inversion during restoration [9,40,41], and inverted vegetation physicochemical indexes [31,35,42]. Further, previous studies have mostly concentrated on farmland economic crops and there have been few studies of coastal wetland plants [43]. Some researchers have used the red edge to study the chlorophyll content of mangroves [24,39,44], but few have used the full-wave-band spectrum as the variable parameter.

In this study, we monitored the hyperspectral values and chlorophyll contents of two species of mangroves during two phases of restoration, short-term and long-term. We use the red-edge position of each sample as the parameter variable, and build a model to estimate the relationship between the variable parameter and the chlorophyll content with simple linear regression. We establish a model of the relationship between the chlorophyll content and full-wave-band spectrum parameters with partial-least-squares (PLS) stepwise regression. We validate the accuracy of the two models. We also compare the new model with the mature red-edge position model to provide a reference for estimating the chlorophyll content of mangroves during different phases of restoration.

## 2. Study Area

The Quanzhou Bay Estuary (24°51'–24°58' N and 118°37'–118°43' E) is at the mouth of the Luoyang River and is a semi-enclosed shallow estuarine bay [45,46] (Figure 1). In October 2003, a provincial-level nature reserve that covered a total area of 7039.56 hm<sup>2</sup> was established in the Quanzhou Bay estuary wetland mainly to protect the mangrove ecosystem, wetland waterfowl, and the habitat. The estuary has a southern subtropical marine monsoon climate and has an annual average temperature of 20.4 °C, annual precipitation of 1120 mm, and the soil salinity ranges from 3.5‰ to 28.9‰. The average high and low-tide levels are 4.83 and 0.31 m, respectively [46]. The Quanzhou Bay estuary has three native mangrove species, *Aegiceras corniculatum*, *Kandelia candel*, and *Avicennia marina*, which form pure stands that extend over a large area [45]. *Aegiceras corniculatum* and *Kandelia candel* are widely used in coastal wetland restoration in this area.

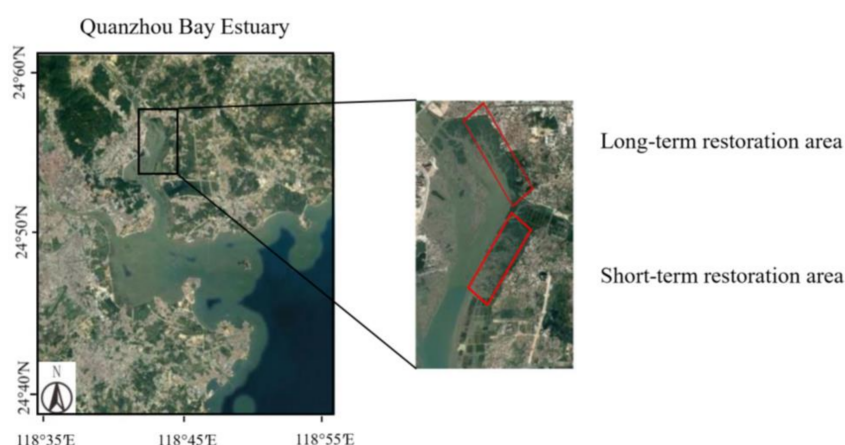


Figure 1. The location of the study area.

## 3. Materials and Methods

### 3.1. Experimental Design

We selected two areas in the nature reserve for our study as follows. A mangrove restoration area was established within the nature reserve in 2003. We chose this area, which now comprises mature mangrove stands, to represent long-term restoration mangroves in our study. The study area comprises another restoration area that was established in 2016 that contains stands of young mangroves, which we selected to examine short-term restoration mangroves. Both areas were planted with *Kandelia candel* and *Aegiceras corniculatum*. *Kandelia candel* is a salt-excluding mangrove species that does not have salt glands on the leaf surface. It isolates the matrix from salt water mainly by maintaining high negative pressure in the xylem. *Aegiceras corniculatum* is a salt-secreting mangrove species with salt glands on the leaf surface that secretes Na and Cl through its leaves to maintain the salt balance. We used leaves of the two mangrove species in the short-term and long-term restoration areas as the control. On 16 November 2017, we collected samples from the shore zone within the Quanzhou Bay estuary wetland nature reserve. The shore zone in

the study area was regarded as a rectangle. We established 3 sampling lines in each study area, each with 60 sampling points (Figure 2). The sampling points were at least 10 m apart, and 180 samples were collected for each type of leaf. The 180 samples were fully representative and met the requirements for the GRAMS IQ software without complicating the analysis. To ensure consistency in the test samples, we collected the second or third leaf on a branch. We used scissors to cut the sample leaves from the plants. The samples were packed in ice bags and transported to a nearby indoor laboratory where they were measured within 2 h. Two-thirds of the samples were used to construct the model and the remaining samples were used to validate it.

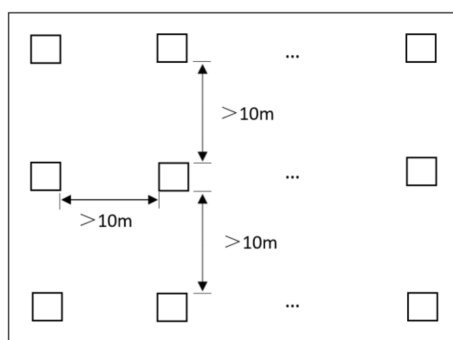


**Figure 2.** Schematic of sampling points.

### 3.2. Leaf Spectrometry

The reflectance spectra of leaves were recorded by an ASD FieldSpec 4 (Analytical Spectral Devices, Inc., Longmont, CO, USA) portable ground object spectrometer. A plant contact probe and leaf clip were used with the spectrometer optical fiber to obtain detailed measurements of the leaf surface (Figure 3). The leaf clip had a double-sided rotatable background plate, a black reference board for measuring leaf reflectivity, and a white reference board for calibration. The spectral parameters are given in Table 1. The leaf was measured directly with an embedded light source (i.e., a built-in halogen lamp). The spectrometer was calibrated before and after measurement with the white reference board, which had a reflectance of 99% [47,48]. The spectral reflectance was obtained by calibrating with the reference board. The spectral reflectance of multiple samples of each leaf type were measured, and 10 curves were drawn with time intervals of 0.1 s. The mean value was used as the spectral reflectance of the sample. For each leaf type, 180 samples were recorded. The spectrometer was calibrated with the white reference board every 15 min.

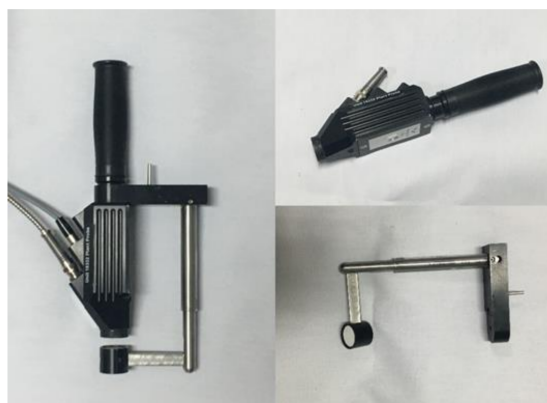


**Figure 3.** Plant contact probe and leaf clip.

**Table 1.** Spectral parameters of the ASD FieldSpec 4.

Parameter Name	Spectral Bands (nm)	Channel Number	Spectral Resolution	Sample Interval	Minimum Integral Time (ms)	Viewing Angle (°)	Standard Illuminant (W)
Parameter values	350~2500	2151	3 nm@700 nm; 10 nm@1400/2100 nm	1.4 nm@350~1000 nm; 1.1 nm@1001~2500 nm	1	25	50

### 3.3. Measurement of the Leaf Chlorophyll Content

Many studies have shown that the Soil and Plant Analyses Development (SPAD) value can accurately represent, and can be used instead of, the content of chlorophyll [49,50]. Immediately after we measured the spectral signals of the leaves, we took SPAD readings with a Chlorophyll Meter SPAD-502 Plus (Konika-Minolta, Inc., Tokyo, Japan) (that gave relative values of between 0 and 100). Measurements were made at five points, namely the leaf tip, above the middle of the leaf, the middle of the leaf, below the middle of the leaf, and the leaf sheath, on the terminal leaflet of the leaf margin [51,52]. We also measured these same leaf parts on each plant. The leaf was sandwiched in the measurement window of the chlorophyll meter, which had a measuring area of 2 mm by 3 mm, and, once stable, the instrument gave the SPAD value. The mean SPAD reading was calculated for each leaf. Measurements were recorded for 180 samples of each leaf type.

### 3.4. Statistical Analyses

Datasets were randomly divided into calibration and validation subsets. Two-thirds of the samples were used to construct the model and the remaining samples were used to validate the model. The full-wave-band spectrum and the red-edge position of each sample were selected as parameter variables. The full-band spectrum covers 2151 subsets between 350 and 2500 nm, and the red-edge area between 660 and 770 nm covers an optimal subset. We used the construction dataset to build estimation models of the relationship between the parameter variables and the SPAD value with PLS stepwise regression and simple linear regression, and then we tested the regression model with the validation dataset. The reflectance spectrum of the red-edge band (660–770 nm) of each sample was intercepted, and the one with the highest reflectance was selected as the variable for constructing the red-edge position model. The computational model derived from the PLS method for the inversion of the chlorophyll content using training samples can be expressed as

$$\text{SPAD} = a_0 + a_1 \times b_1 + \dots + a_n \times b_n$$

where SPAD is the inversion of the chlorophyll content;  $a_0, a_1, \dots, a_n$  are regression coefficients; and  $b_1, \dots, b_n$  are new components calculated from PLS that are linear combinations of the reflectivity in each band. The weight of each component in each band can be used to express the coefficient of each band.

The coefficient of determination ( $R^2$ ) and root-mean-square error (RMSE) were used to assess the predictive performance of the estimation models. The formula for the RMSE is

$$\text{RMSE} = \sqrt{\frac{1}{n} \sum_{i=1}^n (y_i - \hat{y})^2},$$

where  $n$  is the number of observations,  $y_i$  is the measurement,  $\hat{y}$  is the observation, and  $i$  is the simulation label.

## 4. Results

### 4.1. Analysis of the Chlorophyll Content in Samples

We analyzed and compared the data for mangrove leaves from four different conditions. The SPAD values for the chlorophyll content of the short-term restoration of *Kandelia candel* were mainly

between 54 and 88 SPAD, and were between 70 and 85 SPAD for 81% of the samples. The chlorophyll content of the long-term restoration of *Kandelia candel* were relatively uniformly distributed between 39 and 87 SPAD, with the distribution being relatively uniform. The chlorophyll content of the short-term restoration of *Aegiceras corniculatum* were mainly distributed between 45 and 74 SPAD, and 83% of the values were between 55 and 70 SPAD. The chlorophyll content of the long-term restoration of *Aegiceras corniculatum* were mainly between 43 and 68 SPAD, and 91% of the values were between 50 and 65 SPAD. From the average and trend line of the chlorophyll content (see Table 2 and Figure 4), we conclude that the chlorophyll content decreases in the order of the short-term restoration of: *Kandelia candel* > long-term restoration of *Kandelia candel* > short-term restoration of *Aegiceras corniculatum* > long-term restoration of *Aegiceras corniculatum*. The chlorophyll contents of the short-term restoration mangroves were higher than those of the long-term restoration mangroves for both species.

**Table 2.** Statistical analysis of the measured chlorophyll content (SPAD values) in mangrove leaves.

Data Composition	Average (SPAD)	Maximum (SPAD)	Minimum (SPAD)	SD (SPAD)	C.V (%)
Short-term restoration of <i>Kandelia candel</i>	75.7	87.7	54.1	6.2	8.2
Long-term restoration of <i>Kandelia candel</i>	69.7	86.7	39.6	10.3	14.8
Short-term restoration of <i>Aegiceras corniculatum</i>	62.9	73.5	45.2	5.5	8.8
Long-term restoration of <i>Aegiceras corniculatum</i>	56.6	68.0	42.7	4.5	7.9

Note: SD is the standard deviation and the C.V (%) is the coefficient of variation.

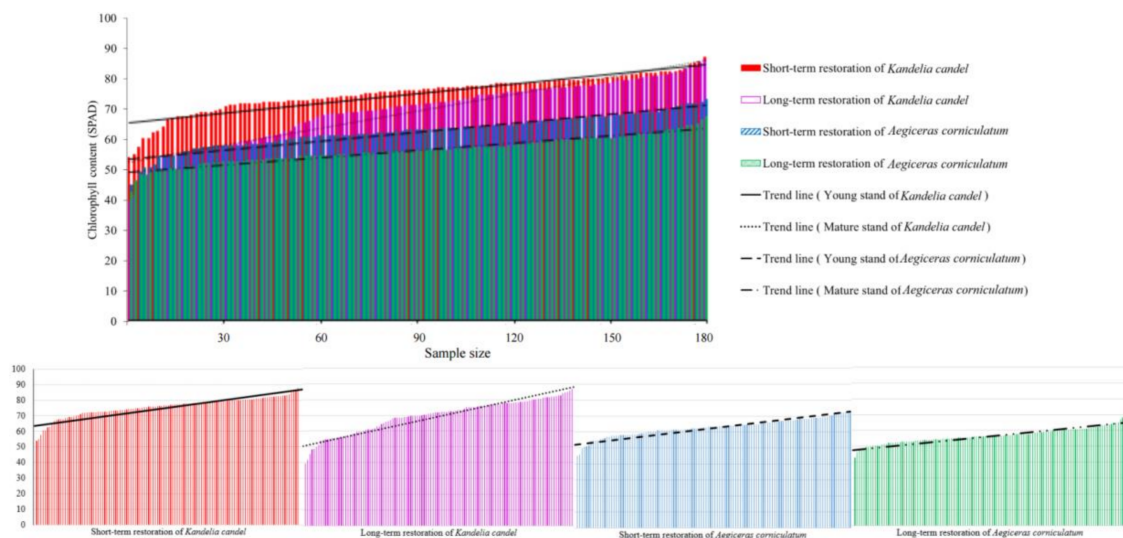


**Figure 4.** Analysis of the chlorophyll content in the mangrove leaves. Samples of leaves from the four conditions are arranged in ascending order of chlorophyll content.

#### 4.2. Comparison of the Spectral Properties of the Mangrove Leaves

The original spectral reflectances of the mangrove leaves ranged from 350 to 2500 nm, as shown in Figure 5. The spectral reflectance curves of the different mangrove leaves coincided in the red light region (620–760 nm). The spectral reflectance curves of the mangrove leaves, both long-term and short-term restorations, show that the reflectance tended to be higher from *Kandelia candel* than *Aegiceras corniculatum*. This was particularly noticeable for the wavelengths between 760 and 1300 nm, where the reflectance of *Kandelia candel* was higher than 0.55 and that of *Aegiceras corniculatum* was lower than 0.55. The spectral reflectance of *Kandelia candel* is higher than that of *Aegiceras corniculatum*. The leaf spectral reflectance curves of long-term restoration and short-term restorations of *Kandelia candel* basically coincided, and there was no obvious difference between the spectral reflectances of the

leaves from short-term and long-term restoration of the same species of mangrove. For *Kandelia candel*, the spectral reflectance from the short-term restoration mangrove was higher than that from the long-term restoration mangrove in most wavelength band regions, while for *Aegiceras corniculatum*, the spectral reflectance from the long-term restoration mangrove was higher than that from the short-term restoration mangrove in most wavelength band regions.

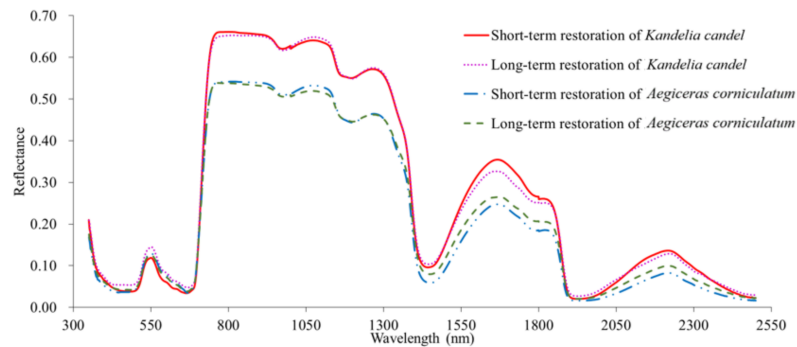


**Figure 5.** Spectral properties of the mangrove leaves (The spectral standard deviations of the mangrove leaves are shown in Supplementary Table S1 at the end of the article).

### 4.3. Model to Estimate the Chlorophyll Content

#### 4.3.1. Red-Edge Position Model

At the red edge, the reflectivity rises sharply because of the intense absorption of vegetation in the red band and multiple scattering of near-infrared radiation within the leaf, resulting in a steep and almost-straight beveled edge. The edge is generally between 660 and 770 nm [53–55]. We investigated the relationship between the location of the red edge and the SPAD value from the spectral measurements and the SPAD values of the mangrove leaves. The chlorophyll content was predicted from a regression equation established between the red-edge position and the SPAD value. The accuracy of the red-edge position model worsened in the order of: long-term restoration of *Kandelia candel* > short-term restoration of *Kandelia candel* > long-term restoration of *Aegiceras corniculatum* > short-term restoration of *Aegiceras corniculatum* (Figure 6).

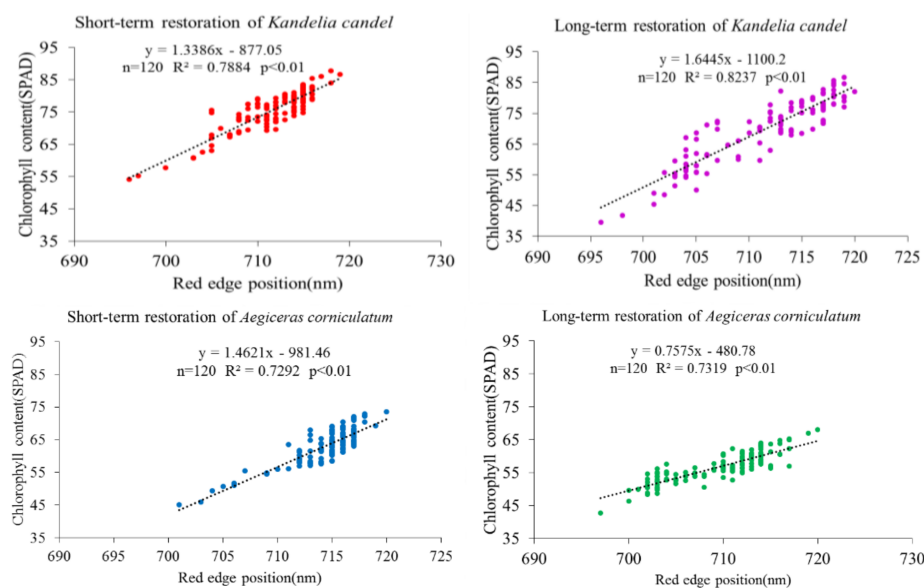


**Figure 6.** Relationship between the chlorophyll content (SPAD values) and the red-edge position.

### 4.3.2. Full-Wave-Band Spectrum Model

Spectral data were first differentiated and reciprocated and then were imported into GRAMS IQ software. Fourier transform, normalization, and multivariate scatter correction were performed on the data with the GRAMS IQ software. From 350 to 2500 nm, the leaves from the four different conditions, corresponding to 2151 spectral units of chlorophyll content, were subjected to factor loading analysis. In Figure 7, which shows the relationship between the spectral units that represented the chlorophyll content of mangrove leaves and the factor loading, we can see that correlations between the spectral representation of the chlorophyll content and the mangrove leaves were similar for the same species of leaf but contrasted for the different leaf species. The crests and troughs of the factor loadings for the mangrove leaves of the two species contrasted at spectral units of 700, 1400, and 1900 nm. This difference may be useful for classifying different mangrove species.

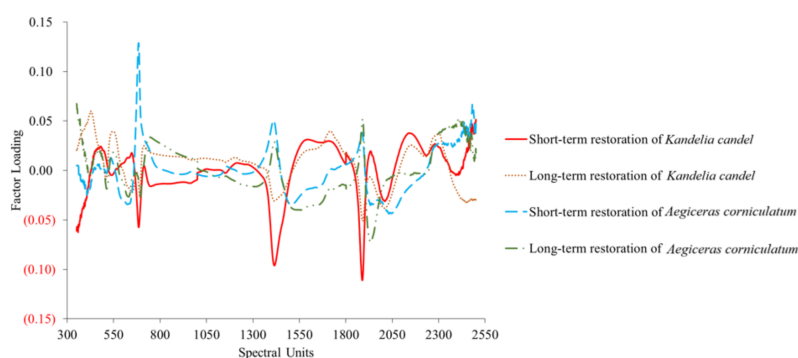


**Figure 7.** Relationship between the chlorophyll content and the spectral unit factor loading of the mangrove leaves.

We used PLS regression to get the best  $R^2$ , and established a model to estimate the chlorophyll content. The full-wave-band spectrum model was more accurate than the red-edge position model. The accuracy of the full-wave-band spectrum model worsened in the order of: long-term restoration of *Kandelia candel* > short-term restoration of *Kandelia candel* > long-term restoration of *Aegiceras corniculatum* > short-term restoration of *Aegiceras corniculatum* (Figure 8).

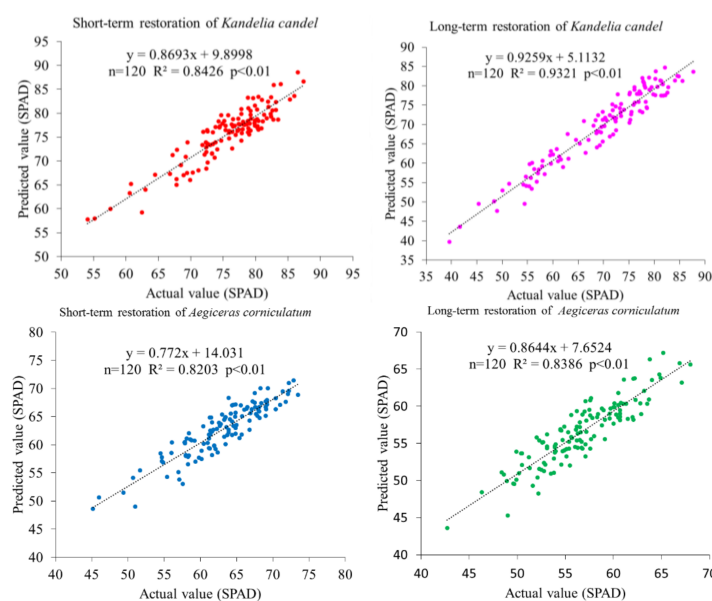


**Figure 8.** Comparison of the observed and predicted values for the full-wave-band spectrum model.

#### 4.4. Verification of the Estimation Model

Sixty sets of sample data were used to validate the model. The  $R^2$  and the RMSE values calculated with the sample data indicated that the accuracy of the full-wave-band spectrum estimation model was high (Figure 9). The coefficients of determination and RMSEs from the regression model for *Kandelia candel* from short-term and long-term restoration were 0.8137 and 0.9353, and 2.47 and 2.26, respectively, while the coefficients of determination and RMSEs for *Aegiceras corniculatum* under short-term and long-term restoration were 0.8296 and 0.8636, and 2.52 and 2.01, respectively. The red-edge position model, with an  $R^2$  value greater than 0.7, was less accurate than the full-wave-band spectrum model (Figure 10).

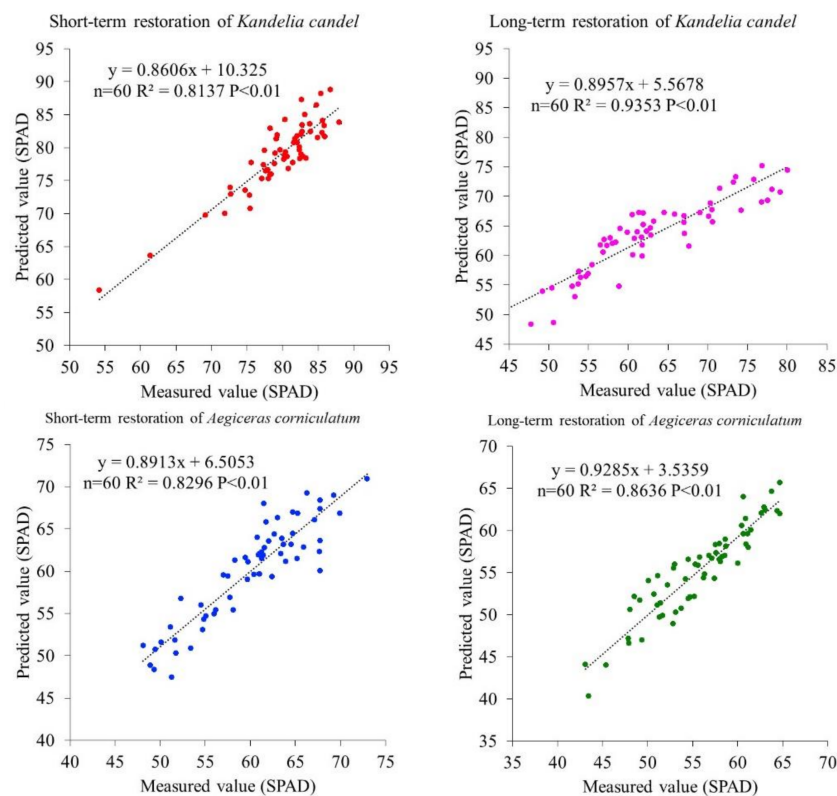


**Figure 9.** Comparison of the observed and predicted values from the full-wave-band spectrum verification model.

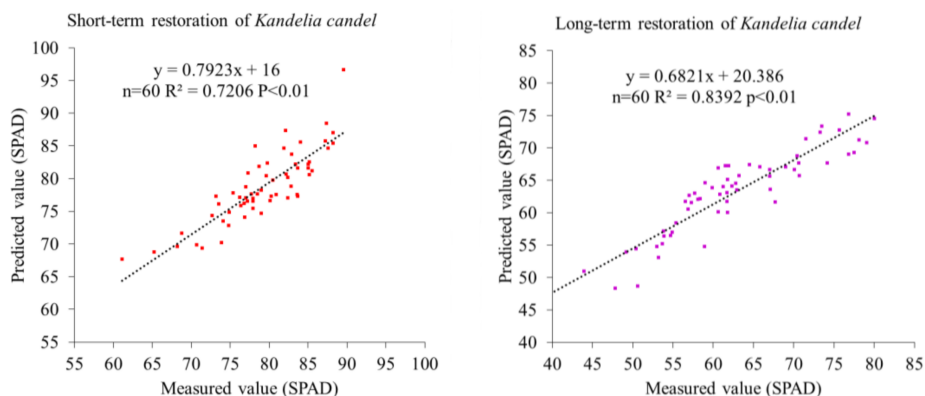


**Figure 10.** Cont.

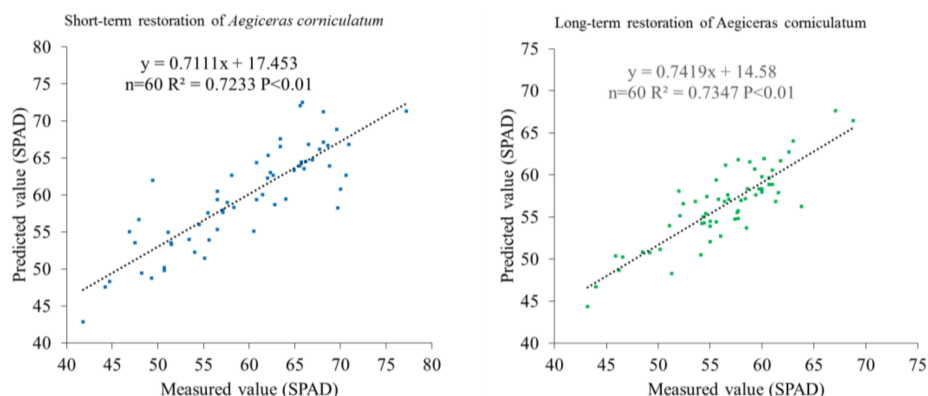


**Figure 10.** Comparison of the observed and predicted values from the red-edge position verification model.

## 5. Discussion

The short-term restoration of *Kandelia candel*, long-term restoration of *Kandelia candel*, short-term restoration of *Aegiceras corniculatum*, and long-term restoration of *Aegiceras corniculatum* had average chlorophyll contents (represented by the SPAD values) of 75.7, 69.7, 62.9, and 56.6, respectively. The leaves from the short-term restoration mangroves had higher chlorophyll contents than those from the long-term restoration mangroves. The short-term restorations mangroves are often submerged in tidal waters and need more chlorophyll for photosynthesis to maintain normal physiological functions [15,56]. Hyperspectral remote sensing can therefore be used to monitor the chlorophyll content of a single species of mangrove in different phases of restoration. When sampling the short-term restoration mangroves, we also found that *Kandelia candel* was more likely to survive in areas frequently submerged by the tide than *Aegiceras corniculatum*. Chen et al. also found that, of a range of mangrove species, *Kandelia candel* had the strongest ability to endure stress in mangrove plantations [57]. Of the short-term restoration mangroves, the average chlorophyll contents (SPAD values) were higher in the *Kandelia candel* than in the *Aegiceras corniculatum*. The higher chlorophyll contents of *Kandelia candel* reflect its stronger photosynthetic ability and stronger survivability, so it may be suitable for planting in coastal mangrove wetland restoration areas that either have a large tidal range or are submerged for long periods.

*Kandelia candel* leaves had a higher spectral reflectance than the *Aegiceras corniculatum* leaves, possibly because *Kandelia candel* is a salt-rejecting mangrove species with isobilateral leaves and no salt glands on the surface, and *Aegiceras corniculatum* is a salt-excluding species with dorsiventral leaves and salt glands on the surface [11,58]. The chlorophyll content is directly related to the intensity of the vegetation photosynthesis and the vegetation vitality, variations in which are reflected in the spectral reflectance curve by the red-edge “red-shift” phenomenon [35,53,55]. In this study, the spectral reflectance curves of the four kinds of mangrove leaf coincided in the region of the red edge, and a red-shift did not occur. We can therefore assume that the vitality of both *Kandelia candel* and *Aegiceras corniculatum* was strong. Our results therefore confirm that, similar to what has been reported by other researchers, hyperspectral data can be used to estimate the chlorophyll content of, and differentiate between, different species [59,60]. As the chlorophyll content is inverted across the whole band, the relationship between the chlorophyll content and the spectral reflectance basically converges for the same species of mangrove leaf but differs considerably for leaves from different mangrove species. Consistent with our finding for *Aegiceras corniculatum*, a salt-secreting species, Ajithkumar et al. found that, as the chlorophyll content in the same species of mangroves (these species were all salt-secreting plants) increased, the spectral reflectance decreased [61]. The spectral reflectance was lower in the short-term restoration mangroves than in the long-term restoration mangroves. However, the opposite was true for *Kandelia candel* (salt-rejecting plants), for which the spectral

reflectance was higher in the short-term restoration mangroves than in the long-term restoration mangroves, perhaps because of variation between the leaf structures of different mangrove species. Flores-de-Santiago et al. found that the spectral reflectance from different species of mangroves varied because of their different chlorophyll contents [24]; these between-species differences may be useful when classifying mangroves.

Both models achieved high estimation accuracy for the same species of mangrove leaves, but the chlorophyll contents estimated by the full-wave-band spectrum model were slightly higher than those from the red-edge position model (Table 3). The inversion results for the chlorophyll content from the red-edge position model in this study were similar to those reported in 2015 by Heenkenda from his examination of the relationship between the observed and predicted chlorophyll values from the Rapid Creek mangrove forest in Darwin, Australia, using the red edge [7]. In 2016, Al-Naimi et al. used the Landsat 8 satellites to estimate the chlorophyll content of mangroves at Al-Khor, Qatar, with a model that had a maximum  $R^2$  value of 0.6016 [62]. In this study, we improved the precision of the model for estimating the chlorophyll content of mangroves. Because the full-wave-band model uses all the band units as variables, it predicts the leaf chlorophyll content more accurately and consistently than the red-edge position model, which has only one variable [63–65]. The validation results further indicate that the full-wave-band spectrum estimation model is more accurate than the red-edge position model, the inversion accuracy of *Kandelia candel* was higher than that of *Aegiceras corniculatum*, and the RMSE of *Aegiceras corniculatum* exceeded 2.96, while that of *Kandelia candel* was less than 2.52. Hyperspectral analysis can therefore be used to retrieve the chlorophyll contents of *Kandelia candel* and *Aegiceras corniculatum*. We found that, when we used the same model to estimate the chlorophyll content of leaves from the same species, the estimates were less accurate for the short-term restoration leaves than for the long-term restoration leaves. The differences among the samples may reflect the frequent flooding of the short-term restoration mangroves, the different distances of the sampling points from the shore, slight variation in the flooding times, and the different degrees of change in the cell structures of the leaves [15,56].

**Table 3.** Comparison of the accuracy of the estimates of the chlorophyll content in mangrove leaves from the two models.

Model	Classification	$R^2$	RMSE	Stat. Sig
Red edge position model	Short-term restoration of <i>Kandelia candel</i>	0.7206	3.11	$p$ -value < 0.01
	Long-term restoration of <i>Kandelia candel</i>	0.8392	3.98	$p$ -value < 0.01
	Short-term restoration of <i>Aegiceras corniculatum</i>	0.7233	4.23	$p$ -value < 0.01
	Long-term restoration of <i>Aegiceras corniculatum</i>	0.7347	2.96	$p$ -value < 0.01
Full-wave band spectrum model	Short-term restoration of <i>Kandelia candel</i>	0.8137	2.47	$p$ -value < 0.01
	Long-term restoration of <i>Kandelia candel</i>	0.9353	2.26	$p$ -value < 0.01
	Short-term restoration of <i>Aegiceras corniculatum</i>	0.8296	2.52	$p$ -value < 0.01
	Long-term restoration of <i>Aegiceras corniculatum</i>	0.8636	2.01	$p$ -value < 0.01

## 6. Conclusions

We examine the relationship between the chlorophyll content and spectral reflectance of mangrove leaves from four different conditions (i.e., leaves from two mangrove species from short-term and long-term restoration areas) using the red-edge position and hyperspectral full-wave-band spectrum as the variable parameters, and establish an optimal model for estimating the chlorophyll content of mangrove leaves.

The spectral reflectance from the mangrove species differ, and the reflectance of *Kandelia candel* is higher than that of *Aegiceras corniculatum*. For the same mangrove species, the spectral reflectance curves are similar at different stages of restoration. Different species of mangroves can be identified by converting the spectrum of hyperspectral data. In the same mangrove species, the chlorophyll contents varies during different restoration stages. We can therefore use the estimates of the chlorophyll content from hyperspectral data to differentiate between stages of restoration.

We establish an empirical model to estimate the chlorophyll content with the red-edge position as the independent variable and achieve a high estimation accuracy. The coefficients of determination of the red-edge position model are 0.7884, 0.8237, 0.7292, and 0.7319 for the short-term restoration of *Kandelia candel*, the long-term restoration of *Kandelia candel*, the short-term restoration of *Aegiceras corniculatum*, and the long-term restoration of *Aegiceras corniculatum*, respectively. These values indicate a good correlation between the red-edge position and the chlorophyll content of mangroves. The full-wave-band spectrum model has coefficients of determination of 0.8426, 0.9321, 0.8203, and 0.8386 for the short-term restoration of *Kandelia candel*, the long-term restoration of *Kandelia candel*, the short-term restoration of *Aegiceras corniculatum*, and the long-term restoration of *Aegiceras corniculatum*, respectively, all of which are higher than the corresponding values for the red-edge position model. The full-wave-band spectrum model therefore gives better estimates of the chlorophyll content of mangrove leaves than the red-edge position model. Our results show that hyperspectral data can be used to estimate the chlorophyll content of mangroves in different phases of restoration.

We analyze the reflectance spectra and chlorophyll contents of mangroves from two stages of restoration (i.e., short-term and long-term restoration) and establish models that can be used to estimate the chlorophyll content in the study area. The estimates can be used as a reference for the chlorophyll content in other mangroves. However, to help us understand the universal significance of this theory, the correlation between the reflectance spectrum data and the chlorophyll content of mangroves at different stages of restoration stage needs to be studied further. We also need further monitoring of mangroves in different restoration stages.

**Supplementary Materials:** The following are available online at <http://www.mdpi.com/2071-1050/10/4/1127/s1>, Table S1: Spectral standard deviation of mangrove leaves (Supplement to Figure 5).

**Acknowledgments:** We acknowledge financial support from the National Key R&D Program of China (2017YFC0506200) and thank Glenn Pennycook, MSc, from Liwen Bianji, Edanz Group China ([www.liwenbianji.cn/ac](http://www.liwenbianji.cn/ac)), for editing the English text of a draft of this manuscript.

**Author Contributions:** Wei Li and Lijuan Cui conceived and designed the experiments; Zhiguo Dou, Wei Li, Jing Li, and Yinuo Zhu performed the experiments and collected the data; Zhiguo Dou, Xincheng Zhao, and Manyin Zhang analyzed the data; Changjun Gao and Xu Pan contributed materials and field work design; and Wei Li, Yinru Lei, and Zhiguo Dou wrote the paper. All authors contributed to various revisions of the article.

**Conflicts of Interest:** The authors declare no conflicts of interest.

## References

1. Chen, B.; Yu, W.; Liu, W.; Liu, Z. An assessment on restoration of typical marine ecosystems in China—Achievements and lessons. *Ocean Coast. Manag.* **2012**, *57*, 53–61. [[CrossRef](#)]
2. Cui, L.; Zhang, M.; Li, W.; Lei, Y.; Ma, M.; Mao, X.; Xiao, H.; Zhao, X. *Understanding Wetlands*; Popular Science Press: Beijing, China, 2017.
3. Huang, G.L. The protection and development of Mangrove Wetland in China. *For. Res. Manag.* **1996**, *5*, 14–17. (In Chinese)
4. Wang, Y.N.; Fu, X.M.; Shao, C.L.; Wang, C.; Li, G.; Liu, G.; Sun, S.; Zeng, X.; Ye, Z.; Guan, S. Investigation on the Status of Mangrove Resources and Medicinal Research in China I. Ecological Functions and Values. *Period. Ocean Univ. China* **2009**, *122*, 2071–2083.
5. Yan, C.; Niu, Z.; Wang, J.; Liu, L.; Huang, J. The assessment of spectral indices applied in chlorophyll content retrieval and a modified crop canopy chlorophyll content retrieval model. *J. Remote Sens.* **2005**, *9*, 742–750.
6. Harahsheh, H. Chapter 4 Remote sensing applications for coastal and marine resources management. *Dev. Earth Environ. Sci.* **2005**, *3*, 49–61.
7. Heenkenda, M.K.; Joyce, K.E.; Maier, S.W.; de Bruin, S. Quantifying mangrove chlorophyll from high spatial resolution imagery. *ISPRS J. Photogramm.* **2015**, *108*, 234–244. [[CrossRef](#)]
8. Guzman, J.P.; Dash, J.; Atkinson, P. Remote sensing of mangrove forest phenology and its environmental drivers. *Remote Sens. Environ.* **2018**, *205*, 71–84. [[CrossRef](#)]

9. Lee, T.M.; Yeh, H.C. Applying remote sensing techniques to monitor shifting wetland vegetation: A case study of Danshui River estuary mangrove communities, Taiwan. *Ecol. Eng.* **2009**, *35*, 487–496. [[CrossRef](#)]
10. Scholander, P.F. How Mangroves Desalinate Seawater. *Physiol. Plant.* **1968**, *21*, 251–261. [[CrossRef](#)]
11. Medina, E.; Fernandez, W.; Barboza, F. Element uptake, accumulation, and resorption in leaves of mangrove species with different mechanisms of salt regulation. *Web Ecol.* **2015**, *15*, 3–13. [[CrossRef](#)]
12. Tomlinson, P.B. *The Botany of Mangroves*; Cambridge University Press: Cambridge, UK, 1986.
13. Lin, P. *Mangroves*; China Ocean Press: Beijing, China, 1984. (In Chinese)
14. Rovai, A.S.; Barufi, J.B.; Pagliosa, P.R.; Scherner, F.; Torres, M.A.; Horta, P.A.; Simonassi, J.C.; Quadros, D.P.; Borges, D.L.; Soriano-Sierra, E.J. Photosynthetic performance of restored and natural mangroves under different environmental constraints. *Environ. Pollut.* **2013**, *181*, 233–241. [[CrossRef](#)] [[PubMed](#)]
15. Zheng, C.; Liu, W.; Qiu, J.; Huang, X.; Chen, S. Comparison of physiological characteristics of *Kandelia obovata*, at different ages in winter in the northernmost mangrove transplanted area of China. *Acta Ecol. Sin.* **2013**, *33*, 132–138. [[CrossRef](#)]
16. Castillo, J.A.A.; Apan, A.; Maraseni, T.N.; Salmo, S. Estimation and mapping of above-ground biomass of mangrove forests and their replacement land uses in the Philippines using Sentinel imagery. *ISPRS J. Photogramm.* **2017**, *134*, 70–85. [[CrossRef](#)]
17. Turpie, K.R.; Klemas, V.V.; Byrd, K.; Kelly, M.; Jo, Y.H. Prospective HypsIRI global observations of tidal wetlands. *Remote Sens. Environ.* **2015**, *167*, 206–217. [[CrossRef](#)]
18. Pham, L.T.H.; Brabyn, L. Monitoring mangrove biomass change in Vietnam using SPOT images and an object-based approach combined with machine learning algorithms. *ISPRS J. Photogramm.* **2017**, *128*, 86–97. [[CrossRef](#)]
19. Vaiphasa, C.; Skidmore, A.K.; Boer, W.F.D.; Vaiphasa, T. A hyperspectral band selector for plant species discrimination. *ISPRS J. Photogramm.* **2007**, *62*, 225–235. [[CrossRef](#)]
20. Zhang, C.; Kovacs, J.; Liu, Y.; Floresverdugo, F.; Floresdesantiago, F. Separating mangrove species and conditions using laboratory hyperspectral data: A case study of a degraded mangrove forest of the Mexican Pacific. *Remote Sens.* **2014**, *6*, 11673–11688. [[CrossRef](#)]
21. Jia, M.; Zhang, Y.; Wang, Z.; Song, K.; Ren, C. Mapping the distribution of mangrove species in the Core Zone of Mai Po Marshes Nature Reserve, Hong Kong, using hyperspectral data and high-resolution data. *Int. J. Appl. Earth Obs.* **2014**, *33*, 226–231. [[CrossRef](#)]
22. Vaiphasa, C.; Ongsomwang, S.; Vaiphasa, T.; Skidmore, A.K. Tropical mangrove species discrimination using hyperspectral data: A laboratory study. *Estuar. Coast. Shelf Sci.* **2005**, *65*, 371–379. [[CrossRef](#)]
23. Reinert, F.; de Pinho, C.F.; Ferreira, M.A. Diagnosing the level of stress on a mangrove species (*Laguncularia racemosa*) contaminated with oil: A necessary step for monitoring mangrove ecosystem. *Mar. Pollut. Bull.* **2016**, *113*, 94–99. [[CrossRef](#)] [[PubMed](#)]
24. Floresdesantiago, F.; Kovacs, J.; Wang, J.; Flores-Verdugo, F.; Zhang, C.; González-Farías, F. Examining the Influence of Seasonality, Condition, and Species Composition on Mangrove Leaf Pigment Contents and Laboratory Based Spectroscopy Data. *Remote Sens.* **2016**, *8*, 226. [[CrossRef](#)]
25. Flores-De-Santiago, F.; Kovacs, J.M.; Flores-Verdugo, F. The influence of seasonality in estimating mangrove leaf chlorophyll—A content from hyperspectral data. *Wetl. Ecol. Manag.* **2013**, *21*, 193–207. [[CrossRef](#)]
26. Das, S. Ecological Restoration and Livelihood: Contribution of Planted Mangroves as Nursery and Habitat for Artisanal and Commercial Fishery. *World Dev.* **2017**, *94*, 492–502. [[CrossRef](#)]
27. Ferreira, A.C.; Ganade, G.; Attayde, J.L.D. Restoration versus natural regeneration in a neotropical mangrove: Effects on plant biomass and crab communities. *Ocean Coast. Manag.* **2015**, *110*, 38–45. [[CrossRef](#)]
28. Stokes, D.J.; Bulmer, R.H.; Lundquist, C.J. Addressing the mismatch between restoration objectives and monitoring needs to support mangrove management. *Ocean Coast. Manag.* **2016**, *134*, 69–78. [[CrossRef](#)]
29. Zaldívar-Jiménez, A.; Ladrón-De-Guevara-Porras, P.; Pérez-Ceballos, R.; Díaz-Mondragón, S.; Rosado-Solórzano, R. US-Mexico joint Gulf of Mexico large marine ecosystem based assessment and management: Experience in community involvement and mangrove wetland restoration in Términos lagoon, Mexico. *Environ. Dev.* **2017**, *22*, 206–213. [[CrossRef](#)]
30. Zarco-Tejada, P.J.; Miller, J.R.; Morales, A.; Berjón, A.; Agüera, J. Hyperspectral indices and model simulation for chlorophyll estimation in open-canopy tree crops. *Remote Sens. Environ.* **2004**, *90*, 463–476. [[CrossRef](#)]
31. Kamal, M.; Phinn, S.; Johansen, K. Assessment of multi-resolution image data for mangrove leaf area index mapping. *Remote Sens. Environ.* **2016**, *176*, 242–254. [[CrossRef](#)]

32. Fauzi, A.; Skidmore, A.K.; Van, G.H.; Schlerf, M.; Heitkönig, I.M.A. Shrimp pond effluent dominates foliar nitrogen in disturbed mangroves as mapped using hyperspectral imagery. *Mar. Pollut. Bull.* **2013**, *76*, 42–51. [[CrossRef](#)] [[PubMed](#)]
33. Cho, M.A.; Skidmore, A.K. A new technique for extracting the red edge position from hyperspectral data: The linear extrapolation method. *Remote Sens. Environ.* **2006**, *101*, 181–193. [[CrossRef](#)]
34. Delegido, J.; Verrelst, J.; Meza, C.M.; Rivera, J.P.; Alonso, L.; Moreno, J. A red-edge spectral index for remote sensing estimation of green LAI over agroecosystems. *Eur. J. Agron.* **2013**, *46*, 42–52. [[CrossRef](#)]
35. Kopačková, V.; Mišurec, J.; Lhotáková, Z.; Oulehle, F.; Albrechtová, J. Using multi-date high spectral resolution data to assess the physiological status of macroscopically undamaged foliage on a regional scale. *Int. J. Appl. Earth Obs.* **2014**, *27*, 169–186. [[CrossRef](#)]
36. Stratoulis, D.; Balzter, H.; Zlinszky, A.; Tóth, V.R. Assessment of ecophysiology of lake shore reed vegetation based on chlorophyll fluorescence, field spectroscopy and hyperspectral airborne imagery. *Remote Sens. Environ.* **2015**, *157*, 72–84. [[CrossRef](#)]
37. Dawson, T.P.; Curran, P.J. Technical note a new technique for interpolating the reflectance red edge position. *Int. J. Remote Sens.* **1998**, *19*, 2133–2139. [[CrossRef](#)]
38. Curran, P.J. Relationship between herbicide concentration during the 1960s and 1970s and the contemporary MERIS Terrestrial Chlorophyll Index (MTCI) for southern Vietnam. *Int. J. Geogr. Inf. Sci.* **2006**, *20*, 929–939.
39. Zhang, C.; Chen, K.; Liu, Y.; Kovacs, J.M.; Flores-Verdugo, F.; Flores-de-Santiago, F. Spectral response to varying levels of leaf pigments collected from a degraded mangrove forest. *J. Appl. Remote Sens.* **2012**, *6*, 063501. [[CrossRef](#)]
40. Cole, B.; Mcmorrow, J.; Evans, M. Empirical Modelling of Vegetation Abundance from Airborne Hyperspectral Data for Upland Peatland Restoration Monitoring. *Remote Sens.* **2014**, *6*, 716–739. [[CrossRef](#)]
41. Möckel, T.; Dalmayne, J.; Prentice, H.; Eklundh, L.; Purschke, O.; Schmidtlein, S.; Hall, K. Classification of Grassland Successional Stages Using Airborne Hyperspectral Imagery. *Remote Sens.* **2014**, *6*, 7732–7761. [[CrossRef](#)]
42. Tian, J.; Wang, L.; Li, X.; Gong, H.; Shi, C.; Zhong, R.; Liu, X. Comparison of UAV and WorldView-2 imagery for mapping leaf area index of mangrove forest. *Int. J. Appl. Earth Obs.* **2017**, *61*, 22–31. [[CrossRef](#)]
43. Li, L.; Ren, T.; Ma, Y.; Wei, Q.; Wang, S.; Li, X.; Cong, R.; Liu, S.; Lu, J. Evaluating chlorophyll density in winter oilseed rape (*Brassica napus* L.) using canopy hyperspectral red-edge parameters. *Comput. Electron. Agric.* **2016**, *126*, 21–31. [[CrossRef](#)]
44. Pastorguzman, J.; Atkinson, P.; Dash, J.; Riojanieto, R. Spatiotemporal Variation in Mangrove Chlorophyll Concentration Using Landsat 8. *Remote Sens.* **2015**, *7*, 14530–14558. [[CrossRef](#)]
45. Li, W.; Cui, L.; Zhang, M.; Wang, Y.; Zhang, Y.; Lei, Y.; Zhao, X. Effect of mangrove restoration on crab burrow density in Luoyangjiang Estuary, China. *For. Ecosyst.* **2015**, *2*, 263–271. [[CrossRef](#)]
46. Fu, W.; Wu, Y. Estimation of aboveground biomass of different mangrove trees based on canopy diameter and tree height. *Procedia Environ. Sci.* **2011**, *10*, 2189–2194. [[CrossRef](#)]
47. Yao, F.; Zhang, Z.; Yang, R.; Sun, J.; Cui, S. Hyperspectral models for estimating vegetation chlorophyll content based on red edge parameter. *Trans. CSAE* **2009**, *25*, 123–129.
48. Croft, H.; Chen, J.M.; Zhang, Y. The applicability of empirical vegetation indices for determining leaf chlorophyll content over different leaf and canopy structures. *Ecol. Complex.* **2014**, *17*, 119–130. [[CrossRef](#)]
49. Delegido, J.; Wittenberghe, S.V.; Verrelst, J.; Ortiz, V.; Veroustraete, F.; Valcke, R.; Samson, R.; Rivera, J.P.; Tenjo, C.; Moreno, J. Chlorophyll content mapping of urban vegetation in the city of Valencia based on the hyperspectral NAOC index. *Ecol. Indic.* **2014**, *40*, 34–42. [[CrossRef](#)]
50. Wang, H.F.; Huo, Z.G.; Zhou, G.S.; Liao, Q.H.; Feng, H.K.; Wu, L. Estimating leaf SPAD values of freeze-damaged winter wheat using continuous wavelet analysis. *Plant Physiol. Biochem.* **2016**, *98*, 39–45. [[CrossRef](#)] [[PubMed](#)]
51. Vos, J.; Bom, M. Hand-held chlorophyll meter: A promising tool to assess the nitrogen status of potato foliage. *Potato Res.* **1993**, *36*, 301–308. [[CrossRef](#)]
52. Wu, J.D.; Wang, D.; Rosen, C.J.; Bauer, M.E. Comparison of petiole nitrate concentrations, SPAD chlorophyll readings, and QuickBird satellite imagery in detecting nitrogen status of potato canopies. *Field Crops Res.* **2015**, *101*, 96–103. [[CrossRef](#)]
53. Curran, P.J.; Dungan, J.L.; Macler, B.A.; Plummer, S.E. The effect of a red leaf pigment on the relationship between red edge and chlorophyll concentration. *Remote Sens. Environ.* **1991**, *35*, 69–76. [[CrossRef](#)]

54. Gates, D.M.; Keegan, H.J.; Schleiter, J.C.; Weidner, V.R. Spectral properties of plants. *Appl. Opt.* **1965**, *4*, 11–20. [[CrossRef](#)]
55. Horler, D.N.H.; Dockray, M.; Barber, J. The red edge of plant leaf reflectance. *Int. J. Remote Sens.* **1983**, *4*, 273–288. [[CrossRef](#)]
56. Ye, Y.; Tam, N.F.Y.; Wong, Y.S.; Lu, C.Y. Growth and physiological responses of two mangrove species (*Bruguiera gymnorhiza*, and *Kandelia candel*) to waterlogging. *Environ. Exp. Bot.* **2003**, *49*, 209–221. [[CrossRef](#)]
57. Chen, L.; Wang, W.; Li, Q.Q.; Zhang, Y.; Yang, S.; Osland, M.J.; Huang, J.; Peng, C. Mangrove species' responses to winter air temperature extremes in China. *Ecosphere* **2017**, *8*, e01865. [[CrossRef](#)]
58. Sahu, S.K.; Singh, R.; Kathiresan, K. Multi-gene phylogenetic analysis reveals the multiple origin and evolution of mangrove physiological traits through exaptation. *Estuar. Coast. Shelf Sci.* **2016**, *183*, 41–51. [[CrossRef](#)]
59. Torrecilla, E.; Stramski, D.; Reynolds, R.A.; Millán-Núñez, E.; Piera, J. Cluster analysis of hyperspectral optical data for discriminating phytoplankton pigment assemblages in the open ocean. *Remote Sens. Environ.* **2011**, *115*, 2578–2593. [[CrossRef](#)]
60. Naidoo, L.; Cho, M.A.; Mathieu, R.; Asner, G. Classification of savanna tree species, in the Greater Kruger National Park region, by integrating hyperspectral and LiDAR data in a Random Forest data mining environment. *ISPRS J. Photogramm.* **2012**, *69*, 167–179. [[CrossRef](#)]
61. Ajithkumar, T.T.; Thangaradjou, T.; Kannan, L. Spectral reflectance properties of mangrove species of the Muthupettai mangrove environment, Tamil Nadu. *J. Environ. Biol.* **2008**, *29*, 785–788. [[PubMed](#)]
62. Al-Naimi, N.; Al-Ghouti, M.A.; Balakrishnan, P. Investigating chlorophyll and nitrogen levels of mangroves at Al-Khor, Qatar: An integrated chemical analysis and remote sensing approach. *Environ. Monit. Assess.* **2016**, *188*, 1–12. [[CrossRef](#)] [[PubMed](#)]
63. Jacquemoud, S.; Baret, F. PROSPECT: A model of leaf optical properties spectra. *Remote Sens. Environ.* **1990**, *34*, 75–91. [[CrossRef](#)]
64. Maier, S.W.; Lüdeker, W.; Günther, K.P. SLOP: A Revised Version of the Stochastic Model for Leaf Optical Properties. *Remote Sens. Environ.* **1999**, *68*, 273–280. [[CrossRef](#)]
65. Féret, J.B.; Gitelson, A.A.; Noble, S.D.; Jacquemoud, S. PROSPECT-D: Towards modeling leaf optical properties through a complete lifecycle. *Remote Sens. Environ.* **2017**, *193*, 204–215. [[CrossRef](#)]



© 2018 by the authors. Licensee MDPI, Basel, Switzerland. This article is an open access article distributed under the terms and conditions of the Creative Commons Attribution (CC BY) license (<http://creativecommons.org/licenses/by/4.0/>).